GEOCHEMICAL MODELLING OF AN INJECTION WELL

Etienne Buscarlet[1], Dario Hernandez[1]

[1]Mighty River Power, PO Box 245, Rotorua 3010, New Zealand

etienne.buscarlet@mightyriver.co.nz

Keywords: *Amorphous silica scaling, reactive transport modeling, Toughreact, specific reactive surface area, injectivity index.*

ABSTRACT

A 1-D radial reactive transport model (TOUGHREACT) is set up to investigate the injection capacity decline in a geothermal injection well. Kinetics data from the existing literature, as well as in-field geologic, chemical and production data are used to define the modeling inputs.

By considering a relationship between porosity and permeability, it is possible to match the injectivity index decline of the injection well (in t/h/bar). The result suggests that the injection capacity decline is related to the permeability reduction in the near-wellbore formation due to amorphous silica deposition. A sensitivity analysis of the relationship between the porosity and permeability and the influence of the specific reactive surface area has been looked into in the model. Several injection options are simulated and their impacts on injection well performance are compared with conventional analytical solutions.

1. INTRODUCTION

Mighty River Power (MRP) operates five geothermal power plants in New Zealand with a total generation capacity of 466 MW. These power plants are located in geothermal fields within the Taupo Volcanic Zone (TVZ) in the North Island.

Deep hot geothermal fluid is used to generate electricity with the processed fluid injected back into the reservoir to maintain reservoir pressure. The injection fluid type depends on the plant design (flash or binary plant), and these can be separated brine, steam condensate or a mixture of both brine and condensate. Therefore the characteristic of the final injection fluid can be significantly different from the produced deep fluid: it is much cooler, and either more concentrated or dilute with respect to dissolved minerals.

Currently, there are two main injection practices being implemented across MRP's operating fields. One is injection of cold fluid (from 90ºC to 130ºC) in a hot geothermal reservoir to induce stimulation and enhance the injection capacity of a well. The cold fluid is either pure steam condensate from a flash plant or separated brine mixed with low-pH dilute steam condensate from a binary plant. The stimulation process is associated with thermal contraction of the rocks causing fractures to open and increasing the near-wellbore permeability (Grant, 2011). In the case of separated brine saturated with silica, the initial stimulation effect on injection capacity usually increases with time until mineral deposition takes over.

The second practice is adding acid to the separated brine to suppress temporarily the polymerization of colloidal silica and prevent scaling across the surface facilities and injection wellbore (Gallup, 1997). However, the pH of the injection fluid is almost immediately buffered once the fluid reaches the reservoir. If the formation temperature around the injection area has been cooled down or is not high enough to heat up the fluid back to saturation level, the amorphous silica will deposit in open spaces of the near-wellbore rocks. The net effect is a reduction in the formation permeability and subsequently the injection well capacity.

Shown in Figure 1 is the injectivity index trend over time of one injection well used by Mighty River Power. This injection well is deviated and was completed in 2009 at around 2900 m total vertical depth with the casing shoe set at ~1500 m. Separated brine has been continuously injected since the end of 2010 and both the injection flow rate and the well head pressure are closely monitored. The injection capacity performance of this well is assessed through its injectivity index (II), calculated as:

$$II = \frac{Q_{inj}}{P_b - P_r}$$ (in Grant and Bixley, 2011),

where Q_{inj} is the injection flow rate (t/h), P_b the pressure in the borehole (bar) and P_r the reservoir pressure (bar).

In absence of downhole pressure tubing, P_b is not known and is commonly calculated from the well head pressure (WHP); by adding the hydrostatic pressure from the surface to the main feedzone less the pressure loss due to friction in the wellbore. For one year and a half of continuous injection, the well injection capacity has shown a significant improvement with an injectivity index (II) increasing close to 230 t/h/bar from the initial value of 130 t/h/bar. After September 2012, the injectivity index has gradually declined to the current value of 50 t/h/bar.

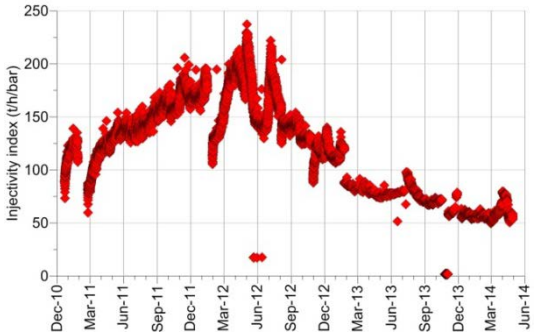

Figure 1: Well injectivity index trend over time.

Given the oversaturation of the injection fluid with respect to amorphous silica (Figure 2, calculated from Fournier, 1989), the likelihood of amorphous silica deposition in the near-well formation is high and most probably responsible for the injectivity index decline. However, it cannot be confirmed as no direct survey was ever conducted in the well to check this assumption.

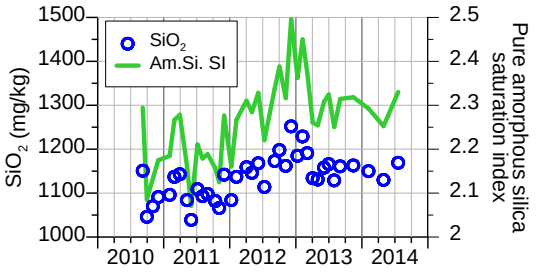

Figure 2: Silica concentration of injection fluid.

The objective of this paper is to model the kinetics of the amorphous silica deposition reactions in the near-well formation and the potential for injection capacity recovery.

2. MODEL SETUP

2.1 Conceptual model

A coupling approach is employed using TOUGHREACT (Xu et al., 2012) to investigate the amorphous silica deposition in the near wellbore formation and its effect on the injection capacity of the well. The modelling approach is based on the work done by Xu et al. (2004) who modelled the scaling of an injection well at Tiwi field in the Philippines.

The period considered in the model covers the life of the injection well (Figure 3). The first part of the modelling period does not consider chemical reactions or transport: the injectivity index increase indicates that thermal stimulation is dominant over chemical precipitation and dissolution processes. The thermal stimulation is mostly associated with geo-mechanical process (Grant, 2011) and cannot be modeled with TOUGHREACT, only pressure and temperature are simulated. The reactive transport associated with changes in porosity and permeability is considered only when the injectivity index starts to decline. At this stage, the deposition and dissolution processes are believed to be dominant and responsible for the decline in injection capacity.

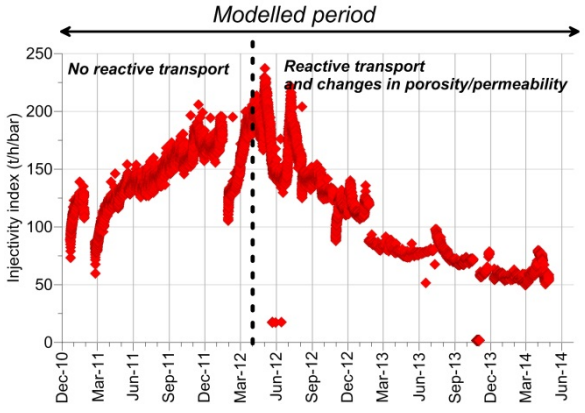

Figure 3: Modeling strategy

2.2 Flow model

A 1-D single phase model was set-up in TOUGHREACT using EOS1 as the equation of state. The model consists of 100 radial blocks with increasing logarithmic size and distributed on a distance of 1000m. The first block is 0.2 m long while the last one is around 100 m long. The thickness of the blocks is 500 m to account for the main feedzones distribution in the well. The last block is set in a fixed-state simulating the reservoir conditions, i.e. P=206 bar and T=320ºC (Figure 4).

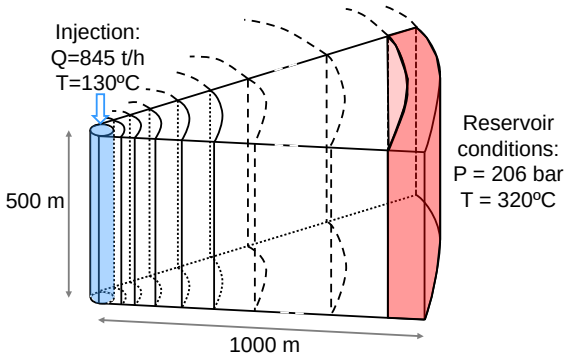

Figure 4: Model schematic

A dual porosity model (MINC) is used, consisting of one matrix layer and one fracture layer having a set of properties as summarized in Table 1. This approach is more appropriate to represent (i) the permeability of the Rotokawa reservoir, which originates mainly from fractures, and (ii) the subsequent heat transfer between the fluid and the reservoir rocks. The modelled connections are fracture-matrix.

Table 1: MINC model properties

	Fracture	Matrix
Fracture spacing (m)	50	-
Permeability (mD)	800	1
Porosity (%)	90	10
Volume (%)	2	98

Water is injected in the facture layer of the first block according to the measured injection flow rate (from 1150 to 845 t/h) at 130ºC. The permeability of the fracture is set at 800 mD, so as to match the injectivity index of ~200 t/h/bar in the injection block prior to the injection capacity decline. It is quite significant but this accounts for the permeability enhancement in the vicinity of the wellbore due to thermal stimulation.

The trends in temperature and pressure based on the model after 1.5 years of continuous injection are presented in Figure 5. All the results presented hereafter are taken from the fracture layer of each block.

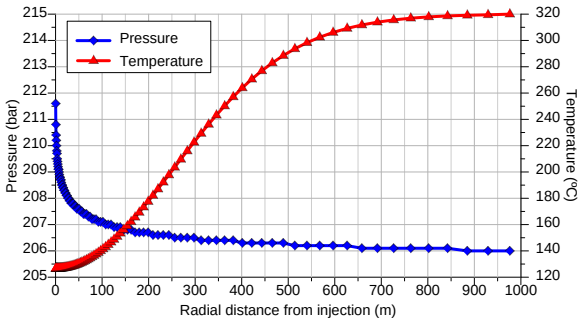

Figure 5: Modeled pressure and temperature after 1.5 years of injection

2.3 Geochemical inputs

The aqueous species and minerals considered in the model are taken from the EQ3/6 database supplied with the TOUGHREACT software. The equilibrium constants are

valid up to 300ºC, yet the simulated temperatures in some blocks of the model are much higher than this (Figure 5). For these blocks the geochemical speciation will be computed as if the temperature is still at 300ºC. The blocks that are outside the thermodynamic temperature range are more than 500 m away from the wellbore and the calculation errors will not affect the model results in the near wellbore. The most significant mechanisms are inferred to take place within the very near-well formation.

Reaction rate

For all the minerals considered in this model, the kinetics of the deposition and dissolution processes are simulated through a surface-controlled reaction of the following form (Referenced in the TOUGHREACT manual, Xu et al, 2012):

$$r = k_{25ºC} exp\left[\frac{-E_a}{R}\left(\frac{1}{T} - \frac{1}{298.15}\right)\right] A\left[1 - \left(\frac{Q}{K}\right)\right]$$

Where r is the rate of deposition and dissolution (mol/m^2/s), $k_{25ºC}$ is the experimental rate constant at 25ºC (for dissolution and/or deposition), E_a is the activation energy (kJ/mol), R the gas constant (J/mol/K), T the temperature (K), A the specific reactive surface area (m^2/kg$_{H2O}$), Q the ion activity product for the reaction and K the equilibrium constant of the reaction. This equation describes the kinetics for most of the minerals. The main uncertainties are the values A and $k_{25ºC}$ and considerable discrepancies exist between laboratory conditions (where most A and $k_{25ºC}$ values are estimated) and field conditions.

For amorphous silica, Carrol et al. (1998) observed from field experiments in Wairakei geothermal field that amorphous silica precipitation rate are in fact 3 times greater than those predicted in theory and the following equation is more realistic for this mineral (implemented in TOUGHREACT):

$$r = k_{25ºC} exp\left[\frac{-E_a}{R}\left(\frac{1}{T} - \frac{1}{298.15}\right)\right] A\left[\left(\frac{Q}{K}\right)^{4.4} - \frac{1}{\left(\frac{Q}{K}\right)^{8.8}}\right]$$

Reactive surface area

The reactive surface area of mineral on the fracture walls can be calculated from the fracture-matrix interface area $A_{f\text{-}m}$ (m^2/m^3) and the true porosity of the rocks $Ø_f$ using the following approximation (Xu et al, 2012):

$$A = \frac{\pi A_{f-m}}{2Ø_f} \text{ in (m}^2\text{/m}^3\text{)}$$

where $A_{f\text{-}m}$ is computed from the TOUGHREACT flow output file. The values for this parameter are small (Table 2). For amorphous silica a much higher value is considered as proposed by Xu et al. (2004) due to the specific colloidal behaviour of the silicic acid in solution and the polymerization process involved in the deposition reaction.

Mineral geochemistry

The mineralogy and abundance of minerals within the formation and implemented in the model were determined from a thin section analysis of a core sample of the injection well collected during drilling (Table 2). The formation rock injected into is mostly andesite with moderate to strong hydrothermal alterations. All the kinetic parameters are taken from Palandri and Kharaka (2004) and consider the same rate for dissolution or deposition.

Table 2: Injection well core sample mineralogy and associated kinetic parameters

Relative abundance of primary and secondary minerals *	Name of equivalent in the LNLL database	Initial volume fraction (%)	Initial reactive specific surface area (m^2/m^3)	Kinetic rate constant at 25ºC (mol/m^2/s)	Activation energy (kJ/mol)
Plagioclase (C)	Maximum microcline (K-feldspar)	5	$1.4x10^{-1}$	$3.9x10^{-13}$	38.0
	Albite-low (Na-feldspar)	5	$1.4x10^{-1}$	$2.7x10^{-13}$	69.8
Chlorite (A)	Clinochlore 7-A	10	$1.4x10^{-1}$	$3.0x10^{-13}$	88.0
Biotite (C)	Muscovite	5	$1.4x10^{-1}$	$2.8x10^{-14}$	22.0
Calcite (C)	Calcite	5	$1.4x10^{-1}$	$2.0x10^{-6}$	23.5
Epidote (C)	Clinozoisite	1	$1.4x10^{-1}$	$1.0x10^{-12}$	70.7
Anhydrite (m)	Anhydrite	0.5	$1.4x10^{-1}$	$6.5x10^{-4}$	14.3
Illite (m)	Illite	0.5	$1.4x10^{-1}$	$3.2x10^{-13}$	58.6
Quartz (m)	Quartz	0.5	$1.4x10^{-1}$	$1.1x10^{-14}$	87.7
Amorphous Silica (nil)	SiO_2(am)	0	$1x10^7$ cm^2/g	$3.8x10^{-10}$	49.8

* Abundant (A) >10%; common (c) 1-10%; minor (m) 0.1-1%; nil: not found

Changes in porosity and permeability

The changes in matrix and fractures porosity are directly tied to volume changes associated with mineral deposition and dissolution. The permeability is in turn modified using a relationship between permeability and porosity. There are two laws considered in this study, both referenced in the TOUGHREACT manual (Xu et al, 2012):

A cubic law: $k = k_i\left(\frac{Ø}{Ø_i}\right)^3$ where k and $Ø$ are the permeability (m^2) the porosity, and k_i and $Ø_i$ their respective initial values. This law assumes a plane parallel fracture of uniform aperture, which may be relevant in this model.

A more complex relationship is given by Verma and Pruess as

$k = k_i\left(\frac{Ø - Ø_c}{Ø_i - Ø_c}\right)^n$ where $Ø_c$ is a critical porosity for which the permeability is zero and n is a power law exponent. Both parameters are determined in the course of the simulation. This law reflects a more realistic relationship based on laboratory experiments.

Aqueous geochemistry

The reservoir natural state fluid chemistry is taken from a nearby well with the historical data processed to reservoir condition using WATCH 2.4 (ISOR, 2013) incorporated into the WATCH automator interface (Zeng, 2013). Most of the relevant chemical parameters are considered such as pH, Ca^{2+}, Mg^{2+}, Na^+. Cl^-, $HCO3^-$, SO_4^{2-}, K^+, Al^{3+} and SiO_2. The calculated reservoir silica concentration is at 720 mg/kg. CO_2 is considered in the model with a partial pressure of 12 bars. The silica concentration of the injection fluid in the model is 1150 mg/kg.

3. MODELLING RESULTS

3.1 Results

The injectivity index is calculated in the first block of the model (referred here as the injection block) and only the fracture layer is considered. The most satisfying fit is obtained using the Verma and Pruess relationship with n=3 and $Ø_c$=0.15 (Figure 6). The cubic law also provides similar outcomes.

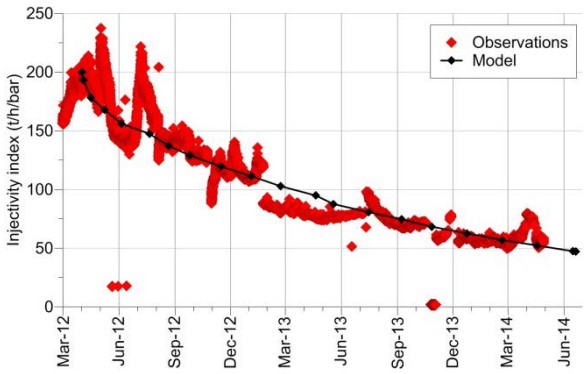

Figure 6: Observed versus modeled II

The model results suggest that a reduction in porosity and permeability occur as silica deposits in the formation. Subsequently, the pressure in the injection block increases as permeability decreases (Figure 7).

At the end of the modelled period, about 0.7 m^3 of silica is deposited in the injection block with the porosity decreased to 70% and permeability reduced by an order of magnitude, from 8.10^{-13} m^2 to 1.10^{-13} m^2.

Unlike the results of Xu et al. (2004), a significant decrease in porosity (~22%) is needed to produce a large permeability reduction (~87%). This is expected as deposition mechanisms and related pressure changes are considered in the fracture layer. No pore throat-clogging effects would happen in this case.

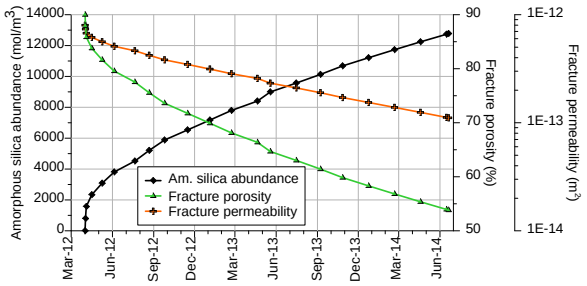

Figure 7: Am. Si. abundance, porosity and permeability versus time

If the chemical reactions were not considered, the pressure in the injection cell would have reached a steady-state (Figure 8).

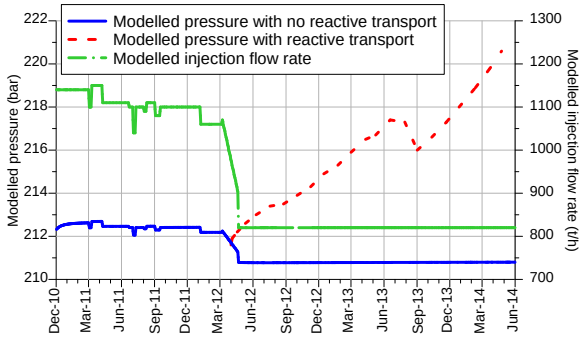

Figure 8: Modelled pressure in the injection block with and without considering the reactive transport

Along the radial plane, the changes associated with silica deposition are restricted within an 80 m radius around the injection block (Figure 9).

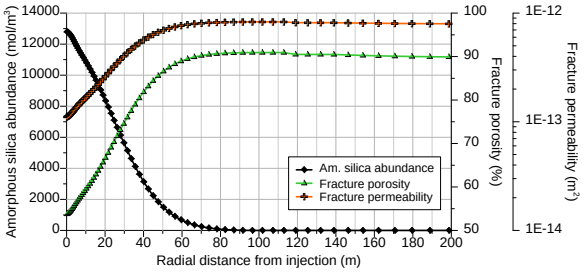

Figure 9: Am. Si. abundance, porosity and permeability after 3.5 years of injection

Considering the chosen kinetic parameters and size of the reactive surface area for the others minerals, the model showed that any significant volumetric changes is controlled by the kinetics of amorphous silica deposition. However, some other processes can be observed as well (Figure 10): injecting cold water will induce dissolution of available calcite, anhydrite and chlorite. All the calcite and anhydrite available in the injection block are entirely dissolved within one month. These dissolution processes may provide some injection capacity enhancement in the absence of amorphous silica deposition. On the other hand, illite and albite are depositing as well (Amount of albite deposited is too small to be plotted here).

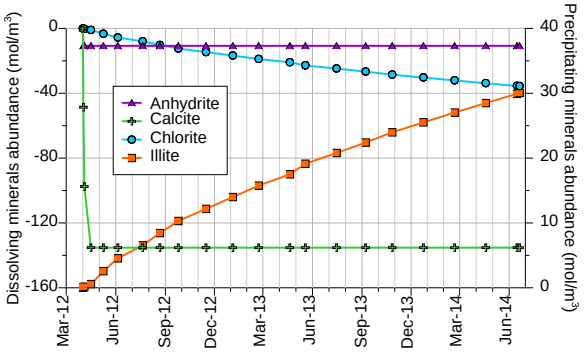

Figure 10: Other minerals kinetics

3.2 Sensitivity analysis on the reactive surface area

In field experiments at Wairakei geothermal field, Carrol et al. (1998) observed that the amorphous silica reaction appeared to be controlled by surface defect/surface nucleation reactions. Considering this result, it is necessary to assess the sensitivity of the reactive surface area parameter in the model. Table 3 gathers values found in the literature. 1000 cm^2/g is a typical value for sand-sized grains while 10 cm^2/g is calculated from a cubic array of truncated spheres. The reactive surface area is somehow an elusive parameter for the geochemical modeller, as can be seen in the range of the values which covers 9 orders of magnitude.

Table 3: Parameters for the sensitivity analysis

Initial reactive specific surface area (cm^2/g)	Source	Verma and Pruess permeability law parameters	
		n	$Ø_C$
$4.8x10^9$	Xu et al. 2012	Cubic law	
$1.0x10^7$ *(initial model)*	Xu et al. 2012	3	0.15
$2.0x10^4$	Bethke, 2011	3	0.25
$1.0x10^3$	Bethke, 2011	3	0.4
$1.0x10^1$	Xu et al. 2012	8	0.8

For each of the simulation considered, parameters for the permeability law were chosen to get the best fit for the observations (Figure 11). The high values of the reactive surface areas (from 2.10^4 to $4.8x10^9$ cm^2/g) provide good results whereas small values (≤1000 cm^2/g) cannot be used to simulate the injectivity index decline.

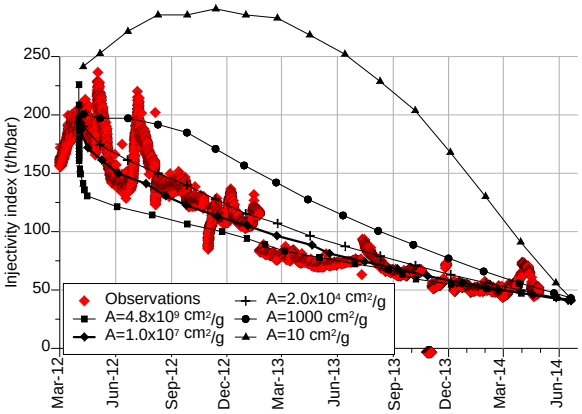

Figure 11: Modeled II for various reactive surface areas

Each model yields different amount of silica, from ~0.06 m^3 for the lowest reactive surface area to 1 m^3 for the highest (Figure 12) at the end of the modeled period, with different changes in the porosity (Figure 13). Less amorphous silica is produced for low reactive surface areas, and the permeability law parameters chosen to make up the porosity decline become irrelevant.

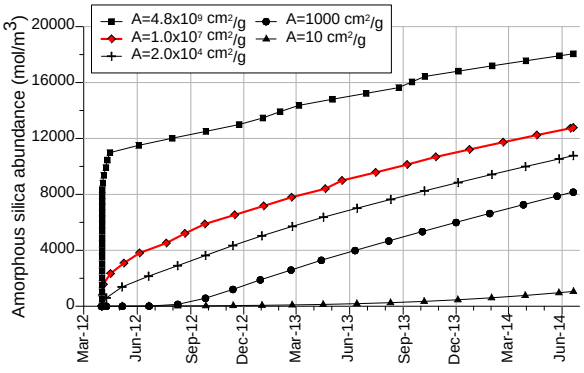

Figure 12: Am. Si. abundance for various reactive surface areas in the injection block

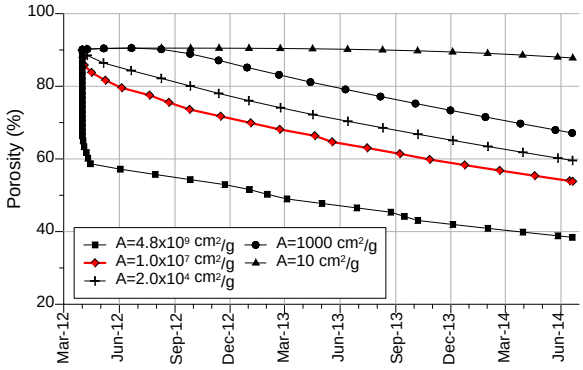

Figure 13: Modeled porosity for various reactive surface areas in the injection block

This sensitivity analysis allows narrowing down the initial broad range of possible values for the reactive surface areas to the high end of the interval.

4. MODEL FORECAST

The initial model is used to investigate the future injection capacity of this well under different injection strategies:

- Option 1: pursue the current injection strategy;
- Option 2: inject a mix of separated brines and condensates, with a lower silica concentration (~720 mg/kg). From a field operational perspective, this option requires a lower flow rate as well (650 t/h);
- Option 3: inject condensates, with silica concentration < 1 ppm and a neutral pH. Similarly the flow rate is lowered to 300 t/h;
- Option 4: pursue the injection of separated brine at half flow-rate (423 t/h).

The results for each simulation are summarized in Figure 14, in terms of amorphous silica deposition/dissolution and the resulting permeability in the injection block. Option 1 leads to a complete failure of the injection well in a 5-years horizon as continuous deposition of amorphous silica decreases the permeability to the point where the flow model is unable to converge. Option 4 has the same outcomes, ruling out the assumption that reducing injection would reduce the scaling rate.

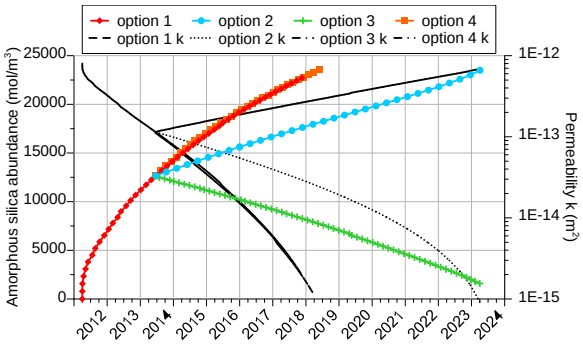

Figure 14: Am. Si. abundance (colored lines) and permeability (black lines) for various injection options

Since the injection fluid in Option 2 is more dilute, the amorphous silica scaling rate is lower. However, failure is predicted in the 10-years horizon as permeability decreases to a point where flow is no longer possible. From an

operational perspective, this would require a higher well-head pressure to inject the same flow rate in the long term and may not be beneficial either for the station operator.

When injecting condensate (Option 3), the fluid in the injection block is undersaturated with amorphous silica and the kinetics is reversed (i.e. amorphous silica is dissolving). After ten years of condensate injection, the injection block will recover some permeability but will not regain its initial permeability value. A large amount of the deposited silica will be dissolved as well. The injection capacity recovery is also lower than the initial decline rate. The initial build-up of illite and albite is not affected by condensate injection.

Comparison of the forecast results for various reactive surface areas provide some interesting outcomes. For Option 1 (Figure 15), all models suggest a well failure in a 2 to 7 years horizon. Larger reactive surface areas promote the deposition reaction at first but tend to minimize the deposition rate as the mineral is building up:

For A=4.8x10^9 cm^2/g, a sharp drop in injectivity index is observed at first but shows a smooth decline slope in the long term. For A=1000 cm^2/g, the decline in injectivity index is slow at first but shows a sharp drop in the long term.

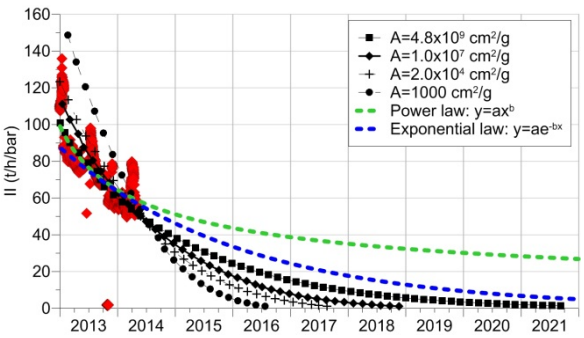

Figure 15: Injectivity index for injection option 1

Two analytical approaches are considered to forecast the injection capacity decline besides chemical considerations: (i) a power law fitted to the whole extent of the decline in injection capacity and (ii) an exponential law fitting the last year of injection capacity decline. When extrapolated, both approaches suggest an injection capacity decline not as rapid as the model results. The outcomes are more optimistic but cannot be validated at present.

Finally the permeability recovery in Option 3 is compared for various reactive surface areas (Figure 16). Similar to Option 1, the lowest reactive surface areas provide the highest rate of reaction and changes in permeability with time. Total recovery relative to the initial permeability is simulated for areas ≤ 20 000 cm^2/g.

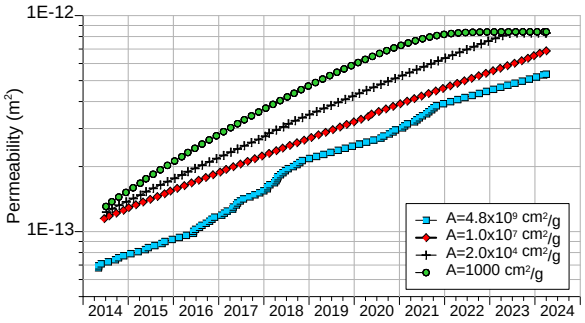

Figure 16: Permeability for injection option 3

5. CONCLUSION

A reactive transport model was set up to simulate the injection capacity decline of an injection well. Thermodynamic data and kinetics parameters were taken from laboratory and field experiments, mainly looking on the amorphous silica.

Although there is no direct field evidence of scaling, the model points to the deposition of amorphous silica in the near-well formation as the likely cause of the injection capacity decline. Using sensible set of parameters it is possible to match accurately the injectivity index decline of the injection well. Sensitive analysis on the reactive surface areas, one of the main uncertainties of the kinetic theory implemented here, provides a range of results which confirms the decline mechanism.

From an operational perspective, several key aspects are suggested from this work. Long-term injection of a fluid highly oversaturated with silica will eventually lead to an injectivity decline. As the near-wellbore formation temperature gets cooler with continuous injection, conditions more and more favourable for the amorphous silica to precipitate are created. Injecting fluid with lower silica content (yet still oversaturated with amorphous silica) provide a temporary relief but just delay the inevitable injectivity decline for a few years.

The mechanism responsible for the decline is restricted in an 80 m radius around the well after 3.5 years of injection. It does not impair the permeability of the surrounding reservoir, and does not affect the targeting of a potential injection make-up well.

The model likewise suggests that replacing a high-silica fluid with a dilute fluid such as plant condensate mitigates the injection capacity decline, and induces some recovery as silica in the near-wellbore is being re-dissolved in the reservoir fluid. However the recovery takes a long time, and over the modelled period (10 years) it was not possible to regain the initial permeability. The model may give some answers if others means of recovery are investigated; e.g. for an acid job, the model provides the likely mineral targets to be dealt with as well as an estimate of the volume of the minerals to be encountered at depth.

One injection strategy for an operator to implement is the periodic switching between separated brine and condensate across injection wells in order to manage their decline and recovery cycles. This will temporarily enhance the injection wells performance in the short term, and delay the immediate need of make-up wells.

AKNOWLEDGEMENTS

The authors wish to thank Farrell Siega (Mighty River Power) for his extensive review of this paper.

REFERENCES

Bethke C., 2011, Geochemical and Biogeochemical Reaction Modeling, Cambridge University Press

Carrol S., Mroczek E., Alai M. and Ebert M., Amorphous silica precipitation (60 to 120ºC): Comparison of laboratory and field rates, Geochemica et Cosmochimica Acta, Vol.62, Nº8, pp. 1379-1396, 1998

Fournier R., 1989, The solubility of silica in hydrothermal solutions: practical applications, UNU-GTP report number 10, 1989

Gallup, D., The Interaction of Silicic Acid with sulfurous acid scale inhibitor, 1997, Geothermal- Resources Council Transactions, Vol. 21, September-October 1997

Grant M., Bixley P., 2011, Geothermal Reservoir Engineering, Academic Press

Iceland GeoSurvey (ISOR), 2013, The Iceland Water Chemistry Group. WATCH software, http://www.geothermal.is/software

Palandri, J.L. and Kharaka, Y.K.: A compilation of rate parameters of water-mineral interaction kinetics for application to geochemical modeling, U.S. Geological Survey (2004)

Xu T., Ontoy Y., Molling P., Spycher N. Parini M. and Pruess K., Reactive transport modeling of an injection well scaling and acidizing at Tiwi field Philippines. Geothermics 33 (2004) 477-491

Xu, T., Sonnenthal, E.,Spycher, N. and Pruess, K.: TOUGHREACT User's Guide: A Simulation Program for Non-isothermal Multiphase Reactive Geochemical Transport in Variably Saturated Porous Media. Lawrence Berkeley National Laboratory, Berkeley, California 94720 (2012)

Zeng Z., Seastres Jr. J. and Mroczek E. (2013): WATCH automator: an excel based data processor for multiple geochemical samples, 35th New Zealand Geothermal Workshop 2013 Proceedings (2005).